

Efficient in Vitro Encapsulation of Protein Cargo by an Engineered Protein Container

Bigna Wörsdörfer, Zbigniew Pianowski, and Donald Hilvert*

Laboratory of Organic Chemistry, ETH Zürich, 8093 Zürich, Switzerland

S Supporting Information

ABSTRACT: An engineered variant of lumazine synthase, a nonviral capsid protein with a negatively charged luminal surface, is shown to encapsulate up to 100 positively supercharged green fluorescent protein (GFP) molecules in vitro. Packaging can be achieved starting either from intact, empty capsids or from capsid fragments by incubation with cargo in aqueous buffer. The yield of encapsulated GFP correlates directly with the host/guest mixing ratio, providing excellent control over packing density. Facile in vitro loading highlights the unusual structural dynamics of this novel nanocontainer and should facilitate diverse biotechnological and materials science applications.

Many proteins spontaneously self-assemble into regular shell-like capsidic structures. Protein capsids are useful, both in nature and in the laboratory, as molecular containers for diverse cargo molecules, ranging from proteins and nucleic acids to metal nanoparticles, quantum dots, and low-molecular-weight drugs. For example, supramolecular inclusion complexes can be employed as delivery vehicles,^{1–4} bioimaging agents,^{5–8} reaction vessels,^{9,10} and templates for the controlled synthesis of novel materials.^{11–14}

Capsids derived from viruses such as the cowpea chlorotic mottle virus and nonviral capsid proteins such as ferritin have been extensively investigated as hosts for encapsulation of specific guest molecules in the laboratory.^{10,15–17} Whereas encapsulation of smaller molecules can often be achieved by diffusion through pores in the capsid shells, for larger molecules, such as proteins or nanoparticles, a different strategy must be adopted. One possibility is chemical or genetic fusion of the cargo molecule to a targeting agent or capsid component that directs localization of the guest to the particle interior during capsid synthesis and assembly in vivo.^{18,19} Spontaneous self-assembly of capsid fragments around the intended guest in vitro, with or without a targeting element, is another alternative.^{9,16,20} The latter approach, which can often be controlled by pH or temperature, is highly versatile, but the yields of encapsulated cargo are typically low.

We previously redesigned a natural capsid-forming enzyme, lumazine synthase from *Aquifex aeolicus* (AaLS), for targeted encapsulation of specific guest proteins in vivo.²¹ Protein engineering was used to introduce negatively charged residues on the luminal surface of the capsid to promote host–guest association with positively charged cargo molecules. The efficacy of this system was demonstrated by successful

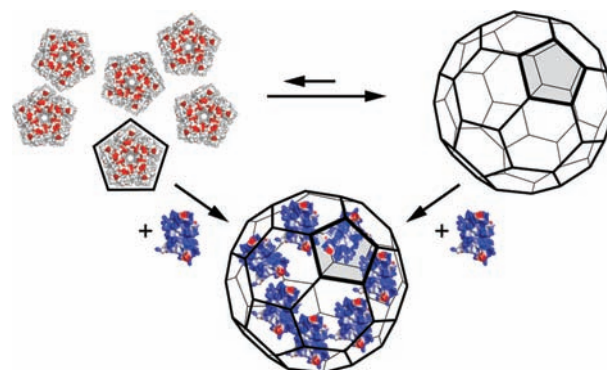


Figure 1. AaLS-13 is produced as a mixture of pentamers and empty capsids. Both forms encapsulate multiple molecules of supercharged GFP(+36) to give highly loaded capsid particles.

sequestration of a toxic protease in the cytosol of *Escherichia coli* and exploitation of the resulting growth advantage to evolve a capsid variant (AaLS-13) with substantially higher loading capacity.²² In this study, we show that the structural dynamics of the evolved capsid protein also enables efficient encapsulation of positively charged guest molecules outside the cell (Figure 1).

For in vitro studies, AaLS-13 was produced cytoplasmically in *E. coli* in the absence of a specific guest and isolated from disrupted cells by Ni²⁺-affinity chromatography. The protein was obtained as a mixture of pentamers, higher-order oligomers, and completely assembled capsids (Figure 2A). The relative ratio of these species depends on the sample concentration and reaction conditions, with the capsid fraction generally increasing over time. The pentamers and small capsid fragments are easily separated from the fully assembled capsids by size-exclusion chromatography. In solution, they slowly but spontaneously assemble to form empty capsids. This process is normally complete within 12 days at room temperature (Figure S1 in the Supporting Information) but can also be accelerated by sonication. Once assembled, the capsids are stable, even upon treatment with ultrasound. Negative-stain electron microscopy (EM) images showed that they adopt symmetric closed-shell structures with an external diameter of 35.9 ± 2.5 nm and an internal diameter of 25.3 ± 1.9 nm (Figure 2B inset), in good agreement with previous measurements.²² These dimensions are consistent with $T = 3$ (180 subunit) icosahedral symmetry.

Received: November 23, 2011

Published: December 22, 2011

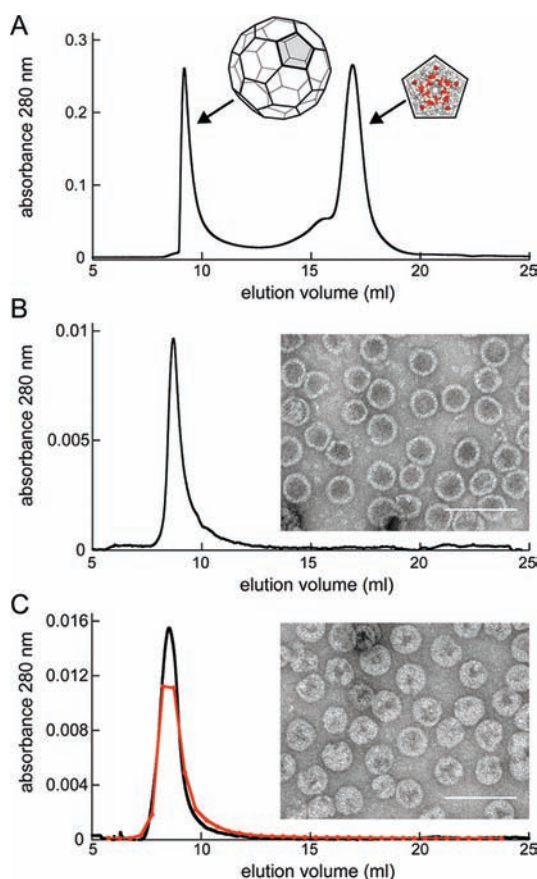


Figure 2. Encapsulation experiments with AaLS-13 capsids: (A) Size-exclusion chromatogram of a freshly isolated AaLS-13 sample consisting of fully assembled capsids, capsid fragments, and smaller oligomers (mostly pentamers). (B) Chromatogram of separated, intact empty capsids. (C) Empty capsids after overnight incubation with GFP(+36) in a 5:1 molar ratio of AaLS-13 monomer to guest. Red: relative fluorescence of individual fractions. The insets in (B) and (C) show EM images of the empty and filled capsid particles, respectively (scale bars 100 nm).

Model encapsulation experiments were carried out with supercharged GFP(+36) (Figure 1), a variant of green fluorescent protein (GFP) in which 29 surface-exposed residues were mutated to positively charged amino acids.²³ Empty capsids were mixed with GFP(+36) at various molar ratios in aqueous buffer (pH 8). Although a 1:1 stoichiometry of AaLS-13 monomer to guest led to immediate coprecipitation of both proteins, a 5-fold excess of AaLS-13 over GFP(+36) afforded a soluble inclusion complex upon overnight incubation. The highly fluorescent AaLS-13 capsids that resulted were isolated by size-exclusion chromatography (Figure 2C). Fluorescence measurements from multiple experiments indicated that GFP(+36) constitutes $39 \pm 4\%$ of the total protein mass in these particles, which corresponds to an average loading of 74 ± 10 GFP molecules per $T = 3$ capsid. This loading level is nearly 6 times higher than that observed when AaLS-13 and GFP(+36) were coproduced *in vivo*.²² Negative-stain EM confirmed the structural integrity of the fluorescent capsids (Figure 2C inset). The loaded capsids are similar in size and shape to the empty structures. However, they have slightly larger external diameters (39.1 ± 2.3 nm) and their lumen is filled with guest molecules. The loading distribution is not uniform, reflecting the stochastic nature of the encapsulation

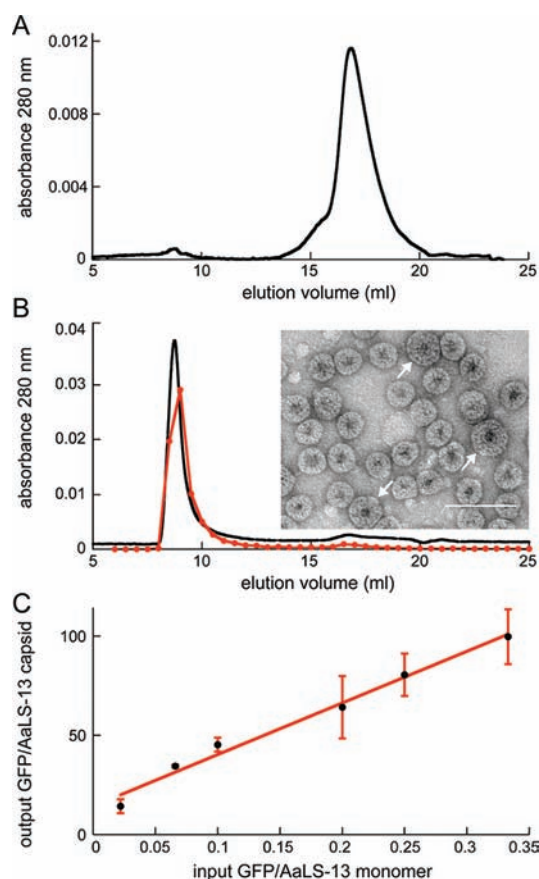


Figure 3. Guest-templated capsid assembly: (A) Size-exclusion chromatogram of isolated and concentrated AaLS-13 capsid fragments. (B) Chromatogram of a sample obtained by mixing capsid fragments with GFP(+36) in a 3:1 ratio after overnight incubation. Red: relative fluorescence of individual fractions. The inset shows an EM image of the packed particles (scale bar 100 nm). The two distinct capsid sizes should be noted. (C) The average number of GFP(+36) molecules per $T = 3$ capsid is linearly proportional to the initial GFP(+36):AaLS-13 mixing ratio.

process, but in all cases, the GFP(+36) molecules localize along the inner walls of the capsid to capitalize on complementary electrostatic interactions with the host. The efficiency of encapsulation suggests that the empty capsids are highly dynamic, readily disassembling to take up guest molecules from the surrounding solution and then reassembling around them. Once guest is bound, the particles become substantially more stable; leakage of GFP(+36) from the host–guest complexes was not observed over 20 days.

Encapsulation can also be accomplished starting from capsid fragments. Mixing AaLS-13 pentamers (Figure 3A) with GFP(+36) in a $\geq 3:1$ molar ratio of AaLS-13 monomer to GFP(+36) cleanly afforded loaded capsid particles (Figure 3B). This process is usually well advanced after 30–60 min and complete after overnight incubation, as judged by size-exclusion chromatography. Loading under these conditions is more uniform than in the experiments with intact capsids. Since qualitatively similar results are obtained when mixtures of intact capsids and capsid fragments are used for encapsulation (Table S1 and Figures S2 and S3), the packaging procedure can be simplified significantly by skipping the size-exclusion step. For both protocols, the number of encapsulated guest molecules is linearly correlated with the original mixing stoichiometry, as

shown by fluorescence measurements (Figure 3C and Table S1) and EM (Figure S3).

The highest encapsulation yields were achieved at 3:1 molar ratios of AaLS-13 monomer to GFP(+36) (Figure 3B). In this case, GFP(+36) constituted $46 \pm 4\%$ of the total protein mass of the recovered particles, which corresponds to 100 ± 14 GFP molecules per $T = 3$ capsid, or a local concentration of ~ 20 mM. For comparison, assuming a packing density of 0.55 for GFP (as in the 1GFL crystal structure in the Protein Data Bank), a GFP volume of 33 nm^3 , and a luminal volume of 8500 nm^3 for the AaLS-13 capsid, we estimate that the $T = 3$ structure could maximally accommodate 140 GFP(+36) molecules. However, the practical loading capacity of this capsid form may be closer to the value observed experimentally and is probably limited by the high surface charge of GFP(+36). Indeed, in contrast to the experiments with lower amounts of guest, a second population of significantly larger loaded capsids was observed in the EM images of these samples. In addition to $38.5 \pm 2.5 \text{ nm}$ diameter structures, roughly 15% of the population consisted of larger capsids with diameters of $48.2 \pm 3.1 \text{ nm}$ (Figure 3B, white arrows). This finding suggests that it may be easier to expand the AaLS-13 capsid to accommodate larger amounts of the supercharged cargo, presumably by a change in T state, than to increase the number of guests in the confined volume of the $T = 3$ structure.

Our results demonstrate that the structural transitions and dynamics of the engineered AaLS-13 capsids can be effectively exploited in vitro to form supramolecular inclusion complexes with complementary positively charged proteins. Controlled loading can be achieved starting from either intact capsids or capsid fragments. In both cases, electrostatic attraction between the host and guest provides the thermodynamic driving force for complex formation. The yield of encapsulated GFP(+36) molecules is generally higher than would be expected from the input ratios (Figure 3C),²⁴ so guest binding must actively template capsid assembly and thus effectively compete with formation of open-shell structures and nonspecific aggregation or precipitation of AaLS-13 fragments.

Biomimetic packaging of cargo molecules in proteinaceous containers is a versatile strategy for generating novel materials,^{11–14} catalysts,^{9,10} and delivery systems.^{1–4} AaLS-13 has already been shown to encapsulate a variety of positively charged proteins in vivo,^{21,22} so we expect that these findings will be readily extendable to other cargo molecules, including positively charged enzymes, nanoparticles with useful optical and magnetic properties, and biologically and medicinally relevant compounds. The controlled formation of densely packed nanocompartments could pave the way to diverse applications in biotechnology and materials science.

■ ASSOCIATED CONTENT

■ Supporting Information

Complete experimental procedures and tables and figures showing dynamics of capsid assembly and loading efficiencies. This material is available free of charge via the Internet at <http://pubs.acs.org>.

■ AUTHOR INFORMATION

Corresponding Author

hilvert@org.chem.ethz.ch

■ ACKNOWLEDGMENTS

We thank M. Lucas and T. Hillmann at the Electron Microscopy Center of the ETH Zürich (EMEZ) for collecting the EM images and assistance with EM data analysis. This work was supported by the Schweizerischer Nationalfond and the ETH Zürich. Z.P. also gratefully acknowledges financial support from the Marie Curie Action within the FP7-PEOPLE Program (IEF-2008-236530).

■ REFERENCES

- (1) Yamada, T.; Iwasaki, Y.; Tada, H.; Iwabuki, H.; Chuah, M. K. L.; van den Driessche, T.; Fukuda, H.; Kondo, A.; Ueda, M.; Seno, M.; Tanizawa, K.; Kuroda, S. *Nat. Biotechnol.* **2003**, *21*, 885–890.
- (2) Abbing, A.; Blaschke, U. K.; Grein, S.; Kretschmar, M.; Stark, C. M. B.; Thies, M. J. W.; Walter, J.; Weigand, M.; Woith, D. C.; Hess, J.; Reiser, C. O. A. *J. Biol. Chem.* **2004**, *279*, 27410–27421.
- (3) Schaffer, D. V.; Koerber, J. T.; Lim, K.-I. *Annu. Rev. Biomed. Eng.* **2008**, *10*, 169–194.
- (4) Stephanopoulos, N.; Tong, G. J.; Hsiao, S. C.; Francis, M. B. *ACS Nano* **2010**, *4*, 6014–6020.
- (5) Aime, S.; Frullano, L.; Geninatti Crich, S. *Angew. Chem., Int. Ed.* **2002**, *41*, 1017–1019.
- (6) Uchida, M.; Flenniken, M. L.; Allen, M.; Willits, D. A.; Crowley, B. E.; Brumfield, S.; Willis, A. F.; Jackiw, L.; Jutila, M.; Young, M. J.; Douglas, T. *J. Am. Chem. Soc.* **2006**, *128*, 16626–16633.
- (7) Hooker, J. M.; Datta, A.; Botta, M.; Raymond, K. N.; Francis, M. B. *Nano Lett.* **2007**, *7*, 2207–2210.
- (8) Liepold, L. O.; Abedin, M. J.; Buckhouse, E. D.; Frank, J. A.; Young, M. J.; Douglas, T. *Nano Lett.* **2009**, *9*, 4520–4526.
- (9) Comellas-Aragonès, M.; Engelkamp, H.; Claessen, V. I.; Sommerdijk, N. A. J. M.; Rowan, A. E.; Christianen, P. C. M.; Maan, J. C.; Verduin, B. J. M.; Cornelissen, J. J. L. M.; Nolte, R. J. M. *Nat. Nanotechnol.* **2007**, *2*, 635–639.
- (10) Bode, S. A.; Minten, I. J.; Nolte, R. J. M.; Cornelissen, J. J. L. M. *Nanoscale* **2011**, *3*, 2376–2389.
- (11) Douglas, T.; Dickson, D. P. E.; Betteridge, S.; Charnock, J.; Garner, C. D.; Mann, S. *Science* **1995**, *269*, 54–57.
- (12) Allen, M.; Willits, D.; Mosolf, J.; Young, M.; Douglas, T. *Adv. Mater.* **2002**, *14*, 1562–1565.
- (13) Chen, C.; Daniel, M. C.; Quinkert, Z. T.; De, M.; Stein, B.; Bowman, V. D.; Chipman, P. R.; Rotello, V. M.; Kao, C. C.; Dragnea, B. *Nano Lett.* **2006**, *6*, 611–615.
- (14) Klem, M. T.; Resnick, D. A.; Gilmore, K.; Young, M.; Idzerda, Y. U.; Douglas, T. *J. Am. Chem. Soc.* **2007**, *129*, 197–201.
- (15) Uchida, M.; Klem, M. T.; Allen, M.; Suci, P.; Flenniken, M.; Gillitzer, E.; Varpness, Z.; Liepold, L. O.; Young, M.; Douglas, T. *Adv. Mater.* **2007**, *19*, 1025–1042.
- (16) Anagyeyi, S. E.; Dufort, C.; Kao, C. C.; Dragnea, B. *J. Mater. Chem.* **2008**, *18*, 3763–3774.
- (17) Uchida, M.; Kang, S.; Reichhardt, C.; Harlen, K.; Douglas, T. *Biochim. Biophys. Acta* **2010**, *1800*, 834–845.
- (18) Fiedler, J. D.; Brown, S. D.; Lau, J. L.; Finn, M. G. *Angew. Chem., Int. Ed.* **2010**, *49*, 9648–9651.
- (19) O'Neil, A.; Reichhardt, C.; Johnson, B.; Prevelige, P. E.; Douglas, T. *Angew. Chem., Int. Ed.* **2011**, *50*, 7425–7428.
- (20) Minten, I. J.; Hendriks, L. J. A.; Nolte, R. J. M.; Cornelissen, J. J. L. M. *J. Am. Chem. Soc.* **2009**, *131*, 17771–17773.
- (21) Seebeck, F. P.; Woycechowsky, K. J.; Zhuang, W.; Rabe, J. P.; Hilvert, D. *J. Am. Chem. Soc.* **2006**, *128*, 4516–4517.
- (22) Wörsdörfer, B.; Woycechowsky, K. J.; Hilvert, D. *Science* **2011**, *331*, 589–592.
- (23) Lawrence, M. S.; Phillips, K. J.; Liu, D. R. *J. Am. Chem. Soc.* **2007**, *129*, 10110–10112.
- (24) For a similar effect with protein-containing vesicles, see: Luisi, P. L.; Allegretti, M.; Pereira de Souza, T.; Steiniger, F.; Fahr, A.; Stano, P. *ChemBioChem* **2010**, *11*, 1989–1992.